

# *In Vitro* Degradation of Poly(L-lactic acid) Fibers Produced by Melt Spinning

A. PEGORETTI, L. FAMBRI, C. MIGLIARESI

Department of Materials Engineering, University of Trento, via Mesiano 77, 38050 Trento, Italy

Received 29 May 1996; accepted 16 August 1996

**ABSTRACT:** *In vitro* degradation of poly(L-lactic acid) fibers was investigated for a period of 16 weeks in Ringer solution at 37°C. Two sets of fibers, with similar initial mechanical properties, molar mass, and crystallinity content, but markedly different in diameter (72 and 120  $\mu\text{m}$ ) were studied. Viscometric molar mass decreased during the immersion time at a faster rate for the thinner fibers compared to the thicker ones. As a consequence, the fiber mechanical properties changed; the elastic modulus was only slightly affected by the molar mass decrease whereas ultimate mechanical properties (stress and strain at break) showed a strong decrease. A quantitative correlation between tensile strength and viscometric-average molar mass was attempted. A possible explanation of the faster degradation rate of the thinner fibers was proposed on the basis of the higher surface/volume ratio and water uptake. Dynamic mechanical properties were also measured as a function of immersion time. © 1997 John Wiley & Sons, Inc. *J Appl Polym Sci* **64**: 213–223, 1997

**Key words:** poly(L-lactic acid); biodegradable fibers; *in vitro* degradation

## INTRODUCTION

Poly(L-lactic acid) (PLLA) is a synthetic, semi-crystalline, biocompatible, and biodegradable polymer<sup>1</sup> that has been widely studied for various biomedical applications such as osteosynthetic devices,<sup>1–5</sup> absorbable sutures,<sup>6</sup> drug delivery implants,<sup>7</sup> and vascular prostheses.<sup>8–10</sup> Simple hydrolysis was recognized as the main mechanism in the degradation process; and a long resorption time, in some cases up to 4 years, was clinically tested *in vivo*. On the other hand, the results of many *in vitro* degradation studies showed that degradation rate depends on many factors, mainly the type of polymer, the processing conditions, and the degradation medium. Crystallinity and/or crystallizability of PLLA is the main factor for

the late degradation kinetics compared to poly(DL-lactic acid) (PDLLA). Moreover, in a previous study<sup>11</sup> the authors showed that even the specimen size, its shape factor, and initial molar mass directly affect the degradation rate. In particular, the lower the surface/volume ratio and the higher the initial molar mass, the slower the degradation rate for the molar mass and the mechanical properties.

In the last few years a great deal of effort has been expended to obtain high strength PLLA fibers for general medical applications by using melt<sup>12–16</sup> or solution<sup>15–26</sup> spinning processes. Starting from good solvents, Gogolewski and Pennings<sup>17</sup> first produced PLLA fibers having tensile strength of 1.2 GPa and later Leenslag and Pennings obtained fibers from a chloroform/toluene mixture having a stress at break up to 2.1 GPa.<sup>19</sup> In a recent study the authors<sup>23</sup> obtained PLLA fibers of about 620,000 viscometric molar mass by a spinning/drawing process using a PLLA/chloro-

Correspondence to: A. Pegoretti (alessandro.pegoretti@ing.unitn.it).

© 1997 John Wiley & Sons, Inc. CCC 0021-8995/97/020213-11

form solution. Mechanical properties of the fibers increased with draw ratio up to tensile modulus and strength of 10 and 1.1 GPa, respectively. The solution-spinning process, however, is not easy to control and for extensive production at the industrial level a melt-extrusion process seems to be indicated. Recently<sup>14</sup> the authors developed and optimized a melt-extrusion/hot-drawing process to obtain PLLA fibers having a tensile strength of 0.87 GPa and a tensile modulus of 9.2 GPa.

Among various possible applications, PLLA fibers were recently proposed for the fabrication of biodegradable medical load-bearing devices, for example, an augmentation device for anterior cruciate ligament reconstruction.<sup>27</sup> Of course for this kind of applications it is extremely important to understand how the fiber mechanical properties depend on their chemical composition, molar mass, porosity, crystallinity, and size. Moreover, in dimensioning a biodegradable device it is necessary to know how the fiber properties change due to the degradation process. Nevertheless, in the literature only a few experimental works exist on the degradation behavior of PLLA fibers.<sup>13,18,24–30</sup>

The aim of this study was to investigate the *in vitro* degradation of PLLA fibers obtained by a melt-extrusion/hot-drawing process.

## EXPERIMENTAL

### Materials

PLLA (RESOMER L 214, Lot 26005), with viscometric molar mass equal to 330,000, was supplied by Boehringer Ingelheim (Germany) and stored in a desiccator under a vacuum until use. A differential scanning calorimetry (DSC) thermogram showed that the melting temperature of the virgin polymer was 187°C and the crystallinity content was 75.3%.

### Fiber Production

Fibers were produced by a two-stage (melt-extrusion and hot-drawing) process. The polymer was melt spun in nitrogen with a laboratory extruder (Friulfiliere, Italy) that had a screw diameter of 14 mm and a cylindrical hole with a diameter of 1.0 mm. A cooling jacket prevented the melting of polymer flakes inside the feed hopper and four heating bands were located along the screw. The extrusion of polymer flakes was performed using

different temperatures along the screw ranging from 200 to 240°C at a constant screw speed of 15 rpm. The as-spun fibers were collected on a glass drum and subsequently drawn at different ratios in nitrogen at a temperature of 160°C with a hot-plate drawing apparatus. The draw ratio has been defined as the ratio between the cross-sectional areas before and after the drawing. The manufacturing process led to a reduction in the average molar mass down to about 100,000. More details about the optimization of the fiber production process are reported elsewhere.<sup>14</sup>

### *In Vitro* Degradation

The degradation of fibers was performed at 37°C in Ringer lactate solution. A commercial solution containing 2.60 g/L of lactic acid, 1.17 g/L of sodium hydroxide, 6.00 g/L of sodium chloride, 0.40 g/L of potassium chloride, and 0.27 g/L of dehydrate calcium chloride was purchased from S.I.-F.R.A. S.p.A. (Isola della Scala, Verona, Italy). The degradation medium was changed every month. The hydrolysis process was followed up to 16 weeks. At each follow-up time, part of the fibers (40–50 mg) were removed from the degradation bath, quickly wiped, and weighted to assess the water uptake. The fibers used for molar mass, mechanical, and thermal measurements were dried under vacuum at 37°C for 24 h.

### Molar Mass Measurements

Molar mass determinations were made by means of viscometric measurements on diluted chloroform/polymer solutions in an Ubbelohde viscometer (type I) at 25.0°C. The viscosity-average molar mass,  $M_v$ , was then calculated from the intrinsic viscosity  $[\eta]$  by using the following equation<sup>31</sup>:

$$[\eta] = 5.45 \times 10^{-4} M_v^{0.73} \quad (1)$$

### Electron Microscopy Investigations

A Cambridge scanning electron microscope (SEM), model Stereoscan 200, was used to observe the surface topography of the fibers. Observations were made at an accelerating voltage of 20 kV.

### DSC Measurements

DSC measurements were conducted using a Mettler DSC 30 calorimeter, covering 0–230°C at

**Table I Initial Properties of PLLA Fibers Before Degradation Test**

	Sample A	Sample B
Diameter ( $\mu\text{m}$ )	120 $\pm$ 10	72 $\pm$ 7
Tensile modulus (GPa)	10.4 $\pm$ 0.4	8.3 $\pm$ 0.6
Stress at break (MPa)	890 $\pm$ 96	968 $\pm$ 105
Yield stress at 0.3% offset (MPa)	242 $\pm$ 12	243 $\pm$ 6
Viscosity-average molar mass	105,900	107,200
Crystallinity content (%)	66.5	66.6

10°C/min in nitrogen flushing at 100 mL/min. Fibers (about 10 mg) were carefully wound around a cylindrical wire (to minimize the stresses due to the sample preparation) and inserted in the aluminum pan of the calorimeter. The crystallization and melting of the specimens was assessed by integrating the normalized area of the exothermal and endothermal peaks, and rating the heat involved to the reference value of the 100% crystalline polymer (93.6 J/g).<sup>32</sup>

### Mechanical Testing

The mechanical properties of the fibers were measured at room temperature by using an Instron tensile tester (model 4502) equipped with a 100N load cell, at a crosshead speed of 12 mm/min. Specimens with a gauge length of 25 mm were prepared using a thin paper test specimen mounting tab as recommended in the ASTM standard D 3379. All the reported tensile properties represent average values of at least five tests.

### Dynamic Mechanical Thermal Analysis (DMTA)

DMTA tests were conducted on a single fiber in the tensile loading mode, by using a Polymer Laboratories dynamic mechanical thermal analyzer (model MkII) with a peak to peak displacement of 16  $\mu\text{m}$ , a frequency of 1 Hz, a temperature range from 0 to 200°C, and a heating rate of 2°C/min.

## RESULTS AND DISCUSSION

Two sets of fibers having similar mechanical properties, viscosity-average molar mass, and crystallinity content, but markedly different diameters were studied. The initial properties of the two sam-

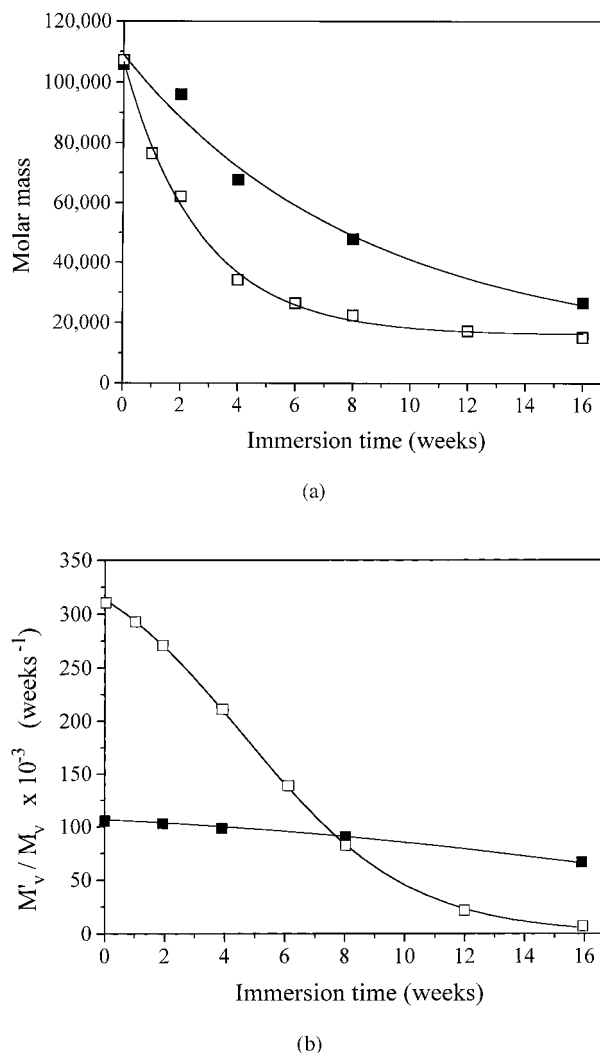


**Figure 1** (a) Effect of immersion time on the viscometric-average molar mass of PLLA fibers of different diameters: (■) 120  $\mu\text{m}$  and (□) 72  $\mu\text{m}$ . (b) Effect of immersion time on the molar mass degradation rate of PLLA fibers of different diameters; symbols as in (a).

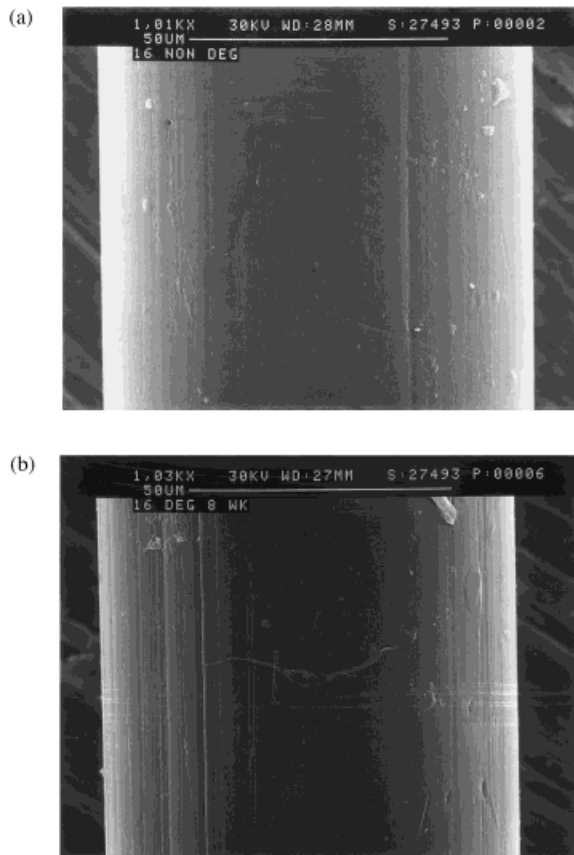


**Figure 2** SEM micrographs (original magnification 1000 $\times$ ) of 72- $\mu\text{m}$  PLLA fibers surface: (a) before the *in vitro* degradation and (b) after 8 weeks of *in vitro* degradation.

ples are reported in Table I. Sample A was obtained from as-spun fibers collected at a speed of 2.2 m/min, having an initial diameter of 440  $\mu\text{m}$  and a quite low crystallinity content (6.5%). On the other hand, sample B was produced starting from different as-spun fibers and collected at a significantly higher speed (5 m/min), resulting in a lower initial diameter (235  $\mu\text{m}$ ) and a higher crystallinity content (29.9%).<sup>14</sup> Both drawn fibers had the same final crystallinity; however, during the hot-drawing stage samples A and B developed 60.0 and 36.7% crystallinity, respectively. Moreover, the distinct melting points, 192 and 178 $^{\circ}\text{C}$ , suggest a different morphology of the crystalline structure. The mechanical properties resulted in values slightly higher than those previously reported for the melt spun fibers,<sup>14</sup> with a maximum elastic modulus of 10.4 GPa and a maximum strength of 968 MPa. The effect of the immersion time on viscometric-average molar mass,  $M_v$ , is reported in

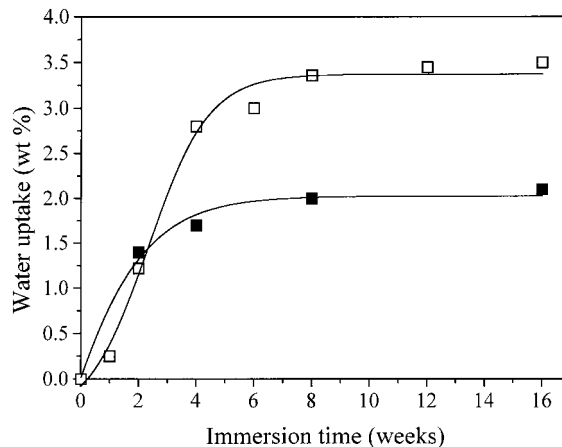


**Figure 3** Water uptake as a function of the immersion time for PLLA fibers with different diameters; symbols as in Figure 1(a).

Figure 1(a). During the degradation period, both samples showed a strong decrease in molar mass with different rates depending on the fiber diameter. To better investigate this phenomenon, a degradation rate,  $M'_v/M_v$  (expressed in weeks<sup>-1</sup>), was defined<sup>11</sup> as the absolute value of the derivative,  $dM_v/dt$  (or  $M'_v$ ), of the best fit function for the molar mass curve normalized to  $M_v$ , the viscometric-average molar mass of the material at time  $t$ . From Figure 1(b) where the degradation rates for both samples are reported as a function of immersion time, the thinner fibers had a higher initial degradation rate ( $314 \times 10^{-3}$  weeks<sup>-1</sup>) in comparison to the thicker one ( $107 \times 10^{-3}$  weeks<sup>-1</sup>). Both data are consistent with the previously reported

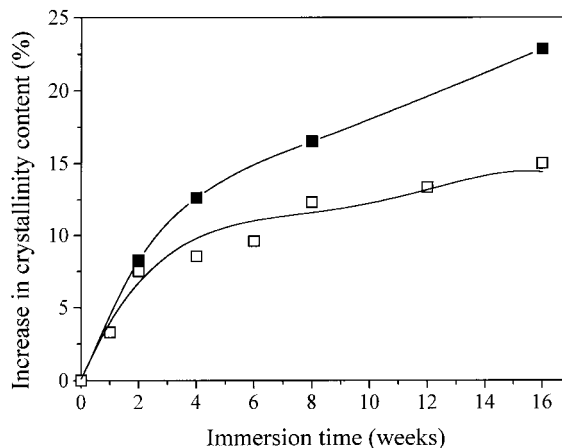


**Figure 4** Increase in crystallinity content as a function of the immersion time for PLLA fibers with different diameters; symbols as in Figure 1(a).

initial degradation rate of bulk PLLA specimens<sup>11</sup> (about  $40 \times 10^{-3}$  weeks<sup>-1</sup>) with their surface to volume ratio much lower than that of the fibers. While the degradation rate of sample A remained practically constant over the entire degradation period, the degradation rate of sample B decreased. After 8 weeks both samples showed the same degradation rate.

The surface topography of both fiber samples was only slightly affected by the degradation process, as clearly evidenced from the SEM micrographs in Figure 2.

From a gravimetric analysis, no mass loss was detected during the whole degradation period, probably because the degraded chains still remained significantly long and showed no water solubility.<sup>11</sup> Nevertheless the fibers were found to absorb a certain amount of water during the degradation process as reported in Figure 3. The higher water uptake of the 72- $\mu$ m fibers can be explained by taking into account the higher surface area and lower crystallinity content of these thinner fibers. As already reported for the *in vitro* degradation of PLLA bulk sample materials,<sup>11</sup> the longer the degradation time, the lower the viscometric molar mass and the higher the crystallinity content. Similarly, the fiber crystallinity content was found to increase during the immersion time, showing almost the same crystallinity con-

tent after 2 weeks; but at longer immersion time the thicker fiber crystallized more than the thinner one, reaching about 82 and 77%, respectively, after 16 weeks (Fig. 4). It is worth noting that, at the same degradation time, crystallinity and viscometric molar mass of the thicker fibers were systematically higher than those of the thinner ones. Moreover, if one compares samples with almost the same  $M_v$  (sample A after 16 weeks and sample B after 6 weeks, for example), the thinner fibers have significantly lower crystallinity. These results seem to contradict the expected correlation between the molar mass and the crystallinity content. A possible explanation of the different crystallization behavior of the two types of PLLA fibers could be related to their different initial morphology, the 120- and 72- $\mu$ m fibers being characterized by draw ratios of 13.4 and 10.6, respectively. The different crystallinity developed during spinning (6.5 vs. 29.9%) and hot drawing (60.0 vs. 36.7%) and the consequent final melting point (192 vs. 178°C) can play a major role in determining a distinct capability to develop further crystallization during the degradation process. Simultaneously the crystallization time of samples with similar  $M_v$  was significantly lower for the thinner fibers: their degradation rate was much higher than the thicker ones. For instance, the 120- $\mu$ m fibers of 67,700 viscometric molar

**Table II** Percent Crystallinity ( $C_m$ ,  $C_{c1}$ ,  $C_{c2}$ ), Melting Temperature ( $T_m$ ), and Crystallization Temperatures ( $T_{c1}$ ,  $T_{c2}$ ) of Samples A and B at Various Degradation Periods

	$M_v$	Scan I			Scan II					
		$T_{mI}$ (°C)	$C_{mI}$ (%)	$T_g$ (°C)	$T_{c1}$ (°C)	$C_{c1}$ (%)	$T_{c2}$ (°C)	$C_{c2}$ (%)	$T_{mII}$ (°C)	$C_{mII}$ (%)
A (weeks)										
0	105,900	192	66.5	64	113	34.7	164	0.3	183	35.0
2	96,000	180	72.0	62	109	41.0	165	2.2	180	43.2
4	67,700	183	74.9	62	109	41.6	166	2.8	181	44.4
8	47,900	182	77.5	61	106	50.2	164	3.6	178	53.8
16	26,600	183	81.7	60	102	54.7	163	3.9	176	58.6
B (weeks)										
0	107,200	178	66.6	62	106	37.0	165	2.6	182	39.6
1	76,500	178	68.8	63	106	40.0	165	2.9	181	42.9
2	62,200	177	71.6	63	110	37.8	165	2.6	182	40.4
4	34,300	176	72.3	62	107	41.3	165	3.6	180	44.9
6	26,500	181	73.0	59	98	51.6	162	3.4	175	55.0
8	22,400	180	74.8	59	99	52.3	161	3.4	174	55.7
12	17,300	179	75.5	58	97	53.0	161	3.2	174	56.2
16	15,100	177	76.6	58	96	53.3	160	1.8	172	55.1

Subscripts I and II refer to the first and second scan, respectively.

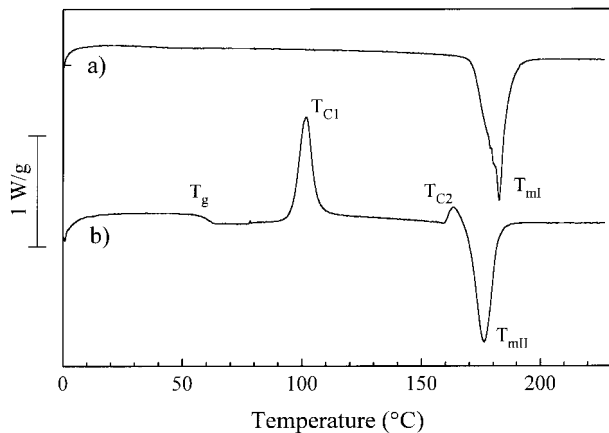


**Figure 5** DSC thermograms of a 120- $\mu\text{m}$  diameter PLLA fiber after a degradation period of 16 weeks: (a) first scan and (b) second scan.

mass changed their crystallinity by 2.6% (from 74.9 to 77.5%) after 4 weeks whereas the 72- $\mu\text{m}$  fibers of 62,200 viscometric molar mass after 4 weeks increased the crystallinity content by only 1.4% (from 71.6 to 73.0%). Now we can also better explain the different water uptake of the two samples. In fact, by comparing Figures 3 and 4, it can be noted that after 4 weeks an almost constant value of water uptake was reached for both fibers samples in correspondence to a slackening in the crystallinity content curve; and in any case, the higher the crystallinity content the lower the water uptake.

Table II summarizes the data obtained from

DSC measurements performed on both samples during the whole degradation period. From the first DSC run we can measure the melting peak temperature  $T_{mI}$  and the amount of crystallinity  $C_{mI}$  of the fibers. The second scan, performed on the sample melted and quenched at a rate of about  $-100^\circ\text{C}/\text{min}$  starting from  $230^\circ\text{C}$ , clearly shows a neat glass transition temperature ( $T_g$ ), a primary crystallization peak at a temperature  $T_{c1}$ , a secondary crystallization peak at a temperature  $T_{c2}$ , and a melting peak at a temperature  $T_{mII}$  (see Fig. 5). From the second scan it is possible to obtain useful information about the material itself, regardless of its previous thermomechanical history. As a consequence of the molar mass decrease, it was possible to observe a reduction of the glass transition temperature and an easier crystallizability as evidenced from the increase in the areas of the crystallization peaks. The lowering of the crystallization ( $T_{c1}$  and  $T_{c2}$ ) and melting ( $T_{mII}$ ) temperatures indicated a minor stability for the crystal structures obtained from shorter polymer chains. Comparing the second DSC scans of fibers with similar  $M_v$ , we confirmed that the degradation process acted in a different way on the 120- and 72- $\mu\text{m}$  fibers. For instance, thicker fibers having  $M_v$  of 26,600 (16 weeks) showed a higher crystallizability ( $C_{c1}$  and  $C_{c2}$ ) and a higher crystallinity ( $C_{mII}$ ) than the thinner fibers having approximately the same viscometric molar mass of 26,500 (6 weeks). This behavior could be interpreted assuming that during degradation 120- $\mu\text{m}$  fibers resulted in a larger molar

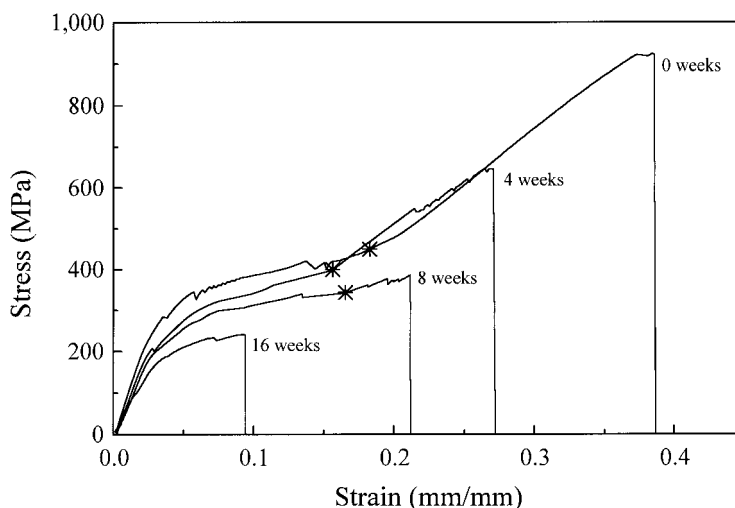


**Figure 6** Stress-strain curves of the 120- $\mu\text{m}$  diameter fiber at various degradation periods. (\*) The point at which strain-hardening occurs.

mass distribution than 72- $\mu\text{m}$  fibers with similar  $M_v$ , thus determining an increase of the crystallizability (shown in Table II).

Figure 6 shows how the overall stress–strain curve of a 120- $\mu\text{m}$  PLLA fiber changed during the immersion period. The behavior of 72- $\mu\text{m}$  fibers was similar. The stress–strain curve of the fiber before the degradation test showed a large plastic deformation after the yield point. The relative low crystallinity of the oriented fiber (about 66%) resulted in about a 34% amorphous phase, which can explain the large plastic deformation presum-

ably related to the number of long chains passing through several crystalline lamellas and amorphous regions.

Moreover, it can be observed that, under the applied test conditions, after a certain point a strain hardening phenomenon<sup>33</sup> occurred that increased the load-bearing capacity of the fibers. This behavior was evident for samples A and B up to a degradation period of 8 weeks, after which the fibers became too brittle as a consequence of the strong molar mass decrease and crystallinity content increase.

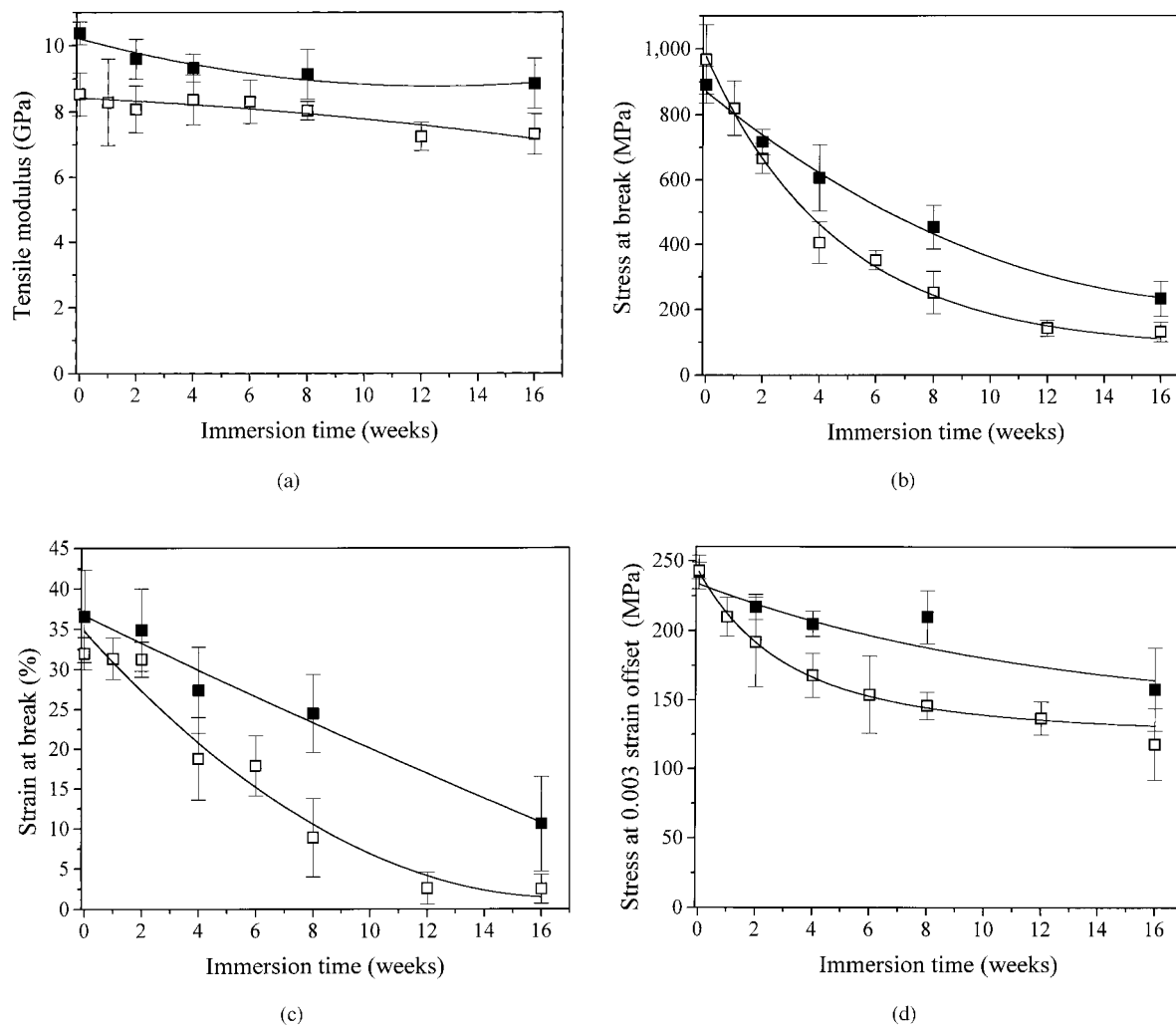


**Figure 7** (a) Tensile Young's modulus as a function of the immersion time for PLLA fibers with different diameters; symbols as in Figure 1(a). (b) Stress at break as a function of the immersion time for PLLA fibers with different diameters; symbols as in Figure 1(a). (c) Strain at break as a function of the immersion time for PLLA fibers with different diameters; symbols as in Figure 1(a). (d) Yield strength at 0.3% offset as a function of the immersion time for PLLA fibers with different diameters; symbols as in Figure 1(a).

Elastic properties were only slightly affected by the molar mass decrease as shown in Figure 7(a), where the values of fibers Young's modulus are reported as a function of immersion time. In fact hydrolysis as well as aging, thermooxidation, static and dynamic fatigue, etc., produced localized damage of the structure on the molecular level; and the influence of such local defects on elastic properties (determined at very small strains) is beyond the accuracy of standard methods. On the other hand ultimate mechanical properties of the polymer rank among the properties that are most sensitive to such structural changes.<sup>34</sup> And in fact, for both samples, stress at break strongly decreased during the immersion period, as can be observed in Figure 7(b). Owing to the faster decrease of molar mass, the thinner fibers lost their tensile strength more rapidly than the thicker ones. Moreover, as can be noted from Figure 6, the fibers became brittle as the degradation proceeded. This behavior is clearly evidenced in Figure 7(c) where the fiber strain at break is reported as a function of the immersion time. Similar to the tensile strength, strain at break of both samples dropped rapidly during degradation.

In most of the clinical applications, biodegradable devices are designed to bear physiological loads with an elastic response. In this regard, it is important to know the stress at which the fiber starts to yield. Figure 6 shows that our PLLA fibers did not show a well-defined yield point; so, as recommended in ASTM standard D 638-89, we evaluated the yield strength as the stress at a specified level of strain offset (we fixed a strain offset of 0.003). The effect of immersion time on the yield strength at 0.003 strain offset is reported in Figure 7(d). As a consequence of the molar mass decrease, yield strength underwent a reduction but at lower rate in comparison to the stress at break. This fact can be explained by considering that, as reported above, the fiber elastic modulus was only slightly affected during the immersion time.

Flory<sup>35</sup> found that the stress at break of cellulose acetate fractions and blends depends on the number-average molar mass,  $M_n$ , according to the following equation:

$$\sigma_b = \sigma_b(\infty) - \frac{K}{M_n} \quad (2)$$

where  $\sigma_b(\infty)$  is the limiting tensile strength for very high molar mass<sup>36</sup> and  $K$  is a constant evaluated

with the aid of experimental data. Although eq. (2) was found to be valid for polymeric materials undergoing brittle fracture,<sup>37</sup> it seems to be quite general.<sup>38</sup> For PLLA fibers with relatively narrow molecular weight distribution, one can use  $M_v$  instead of  $M_n$  as reported by Eling et al.<sup>15</sup> In particular they found that the tensile strength of PLLA fibers, with various viscometric-average molar masses in the range 180,000–530,000, follows eq. (2) only for  $M_v$  values higher than about 300,000. In our case the stress at break of the two fiber samples before and after degradation is reported in Figure 8 as a function of the reciprocal of the viscosity-average molar mass. Similar to the behavior reported in the literature for the brittle strength of several polyethylene samples,<sup>39</sup> we found that our experimental data obey eq. (2) plausibly well over a range of  $M_v$  values higher than about 50,000. The extrapolated value for the limiting tensile strength was equal to about 1.23 GPa, which could be assumed as the upper theoretical limit for the tensile strength of PLLA fibers produced by the melt-spinning procedure. It is interesting to observe that if we plot the stress at which the fibers start their strain-hardening process and the stress at break of the fibers undergoing brittle fracture as a function of the reciprocal of the viscosity-average molar mass, we obtain an almost linear relationship, in accordance with eq. (2).

PLLA fiber dynamic mechanical properties were influenced by the *in vitro* degradation at 37°C. In Figure 9(a) we report tensile storage

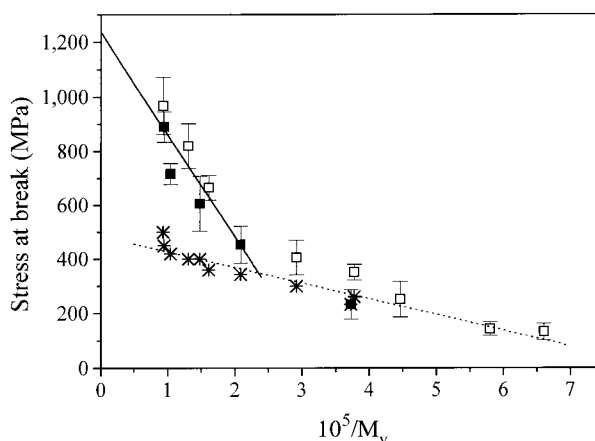


**Figure 8** Stress at break as a function of the reciprocal of the viscosity-average molar mass for PLLA fibers with different diameters; symbols as in Figure 1(a). (\*) Stress at which strain-hardening occurs is also reported.



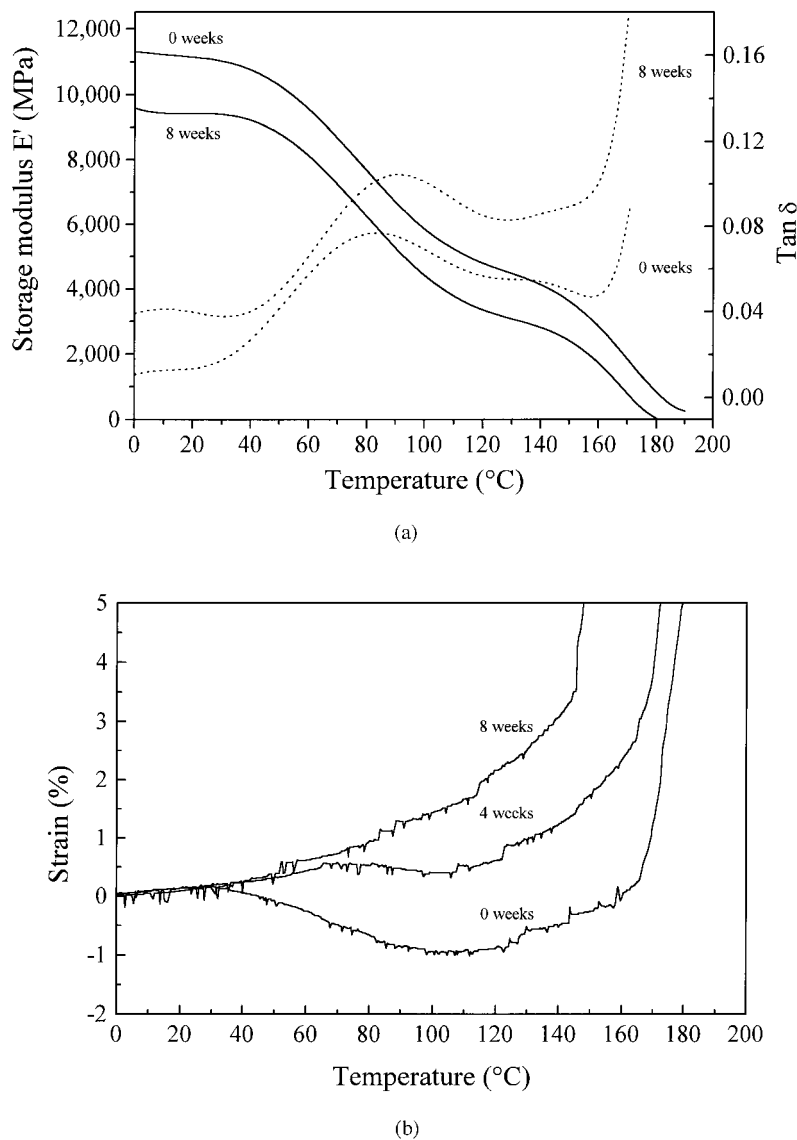


**Figure 9** (a) Dynamic tensile storage modulus ( $E'$ ) and  $\tan \delta$  curves as a function of temperature for the 120- $\mu\text{m}$  diameter fiber at various degradation periods. (b) Sample strain as a function of test temperature during DMTA measurement in tensile mode for the 120- $\mu\text{m}$  diameter fiber at various degradation periods.

modulus ( $E'$ ) and loss factor ( $\tan \delta$ ) as a function of temperature at different degradation periods for a 120- $\mu\text{m}$  fiber. As the degradation proceeded, the fiber showed a slight decrease of tensile  $E'$ . The damping was strongly dependent upon molar mass. In particular, the values of the loss factor above  $T_g$  increased as the molar mass decreased. This behavior is in accordance with previous observations reported by Nielsen.<sup>40</sup> From DMTA tests in tensile mode it was possible to measure the sample strain under the cyclic loading. Figure

9(b) shows the strain under a mean load of 0.1N for a 120- $\mu\text{m}$  fiber after various immersion periods as a function of the test temperature. From Figure 9(b) it is possible to observe that prior to the *in vitro* degradation, the fiber shrunk during the DMTA thermal run in a temperature range from about 40 to 170 $^{\circ}\text{C}$ . After 4 weeks of degradation, the fiber shrinkage became less pronounced; after 8 weeks of immersion, the fiber did not show any thermal contraction. This behavior suggests that during the immersion in the Ringer solution at

37°C, the fibers relaxed the frozen residual strains developed during the hot-drawing process. Given that, Figure 9(b) demonstrates how the degradation process reduced the fiber thermal stability, that is, the temperature at which the fiber started its unstable elongation.

## CONCLUSIONS

*In vitro* hydrolytic degradation of melt spun PLLA fibers in Ringer solution at 37°C caused a strong decrease of the viscometric-average molar mass, resulting in a remarkable loss of mechanical properties. In fact, whereas fiber elastic modulus was only slightly influenced by the degradation process, stress and strain at break fell below 20% of the initial values after a degradation period of 16 weeks. Thinner fibers degraded faster than the thicker ones, as far as molar mass and mechanical properties are concerned. As the degradation proceeded, the fiber crystallinity content and water uptake were found to increase. In particular, the thicker fibers showed a higher increase in crystallinity content and a lower water uptake with respect to the thinner one, further supporting the observed slower reduction of the mechanical properties. The main reason for the different degradation behavior was tentatively attributed to the different surface/volume ratio of the fibers. DMTA measurements showed that during degradation the tensile storage modulus slightly decreased and the damping values increased.

A theoretical upper limit for the tensile strength of melt spun fibers, determined by extrapolation of experimental values, was assessed to be about 1.23 GPa.

In conclusion, it was shown that high strength PLLA fibers produced in different conditions of melt spinning and hot drawing, and having very similar initial properties, behaved differently during *in vitro* degradation.

This work was partly supported by CNR (Comitato Nazionale Tecnologie e Innovazione, Progetto Strategico Materiali Innovativi) and Cremascoli S.r.l. (Milano, Italy).

## REFERENCES

1. F. R. Rozema, Ph.D. Thesis, University of Groningen, Groningen, The Netherlands, 1991, Chap. 1.
2. J. W. Leeslag, A. J. Pennings, R. R. M. Bos, F. R. Rozema, and G. Boering, *Biomaterials*, **8**, 70 (1987).
3. M. Vert, P. Christel, H. Garreau, M. Audion, M. Chavanaz, and F. Chabot, in *Polymers in Medicine II: Biomedical and Pharmaceutical Applications*, E. Chiellini, P. Giusti, C. Migliaresi, and L. Nicolais, Eds., Plenum Press, New York, 1986, p. 263.
4. D. G. Tunc, *Clin. Mater.*, **8**, 119 (1991).
5. K. L. Gerlach, *Clin. Mater.*, **13**, 21 (1993).
6. B. C. Benicewicz and P. K. Hopper, *J. Bioact. Compat. Polym.*, **6**, 64 (1991).
7. D. H. Lewis, in *Biodegradable Polymers as Drug Delivery Systems*, M. Chasin and R. Langer, Eds., Marcel Dekker, New York, 1990, p. 1.
8. J. W. Leeslag, M. T. Kroes, A. J. Pennings, and B. Van der Lei, *New Polym. Mater.*, **1**, 111 (1988).
9. E. Lommen, S. Gogolewski, A. J. Pennings, C. R. H. Winderuur, and P. Nienwenhuis, *Trans. ASAIO*, **29**, 255 (1983).
10. C. M. Agrawal, K. F. Haas, D. A. Leopold, and H. G. Clark, *Biomaterials*, **13**, 176 (1992).
11. C. Migliaresi, L. Fambri, and D. Cohn, *J. Biomater. Sci. Polym. Ed.*, **5**, 591 (1994).
12. R. K. Kulkarni, E. G. Moore, A. F. Hegyeli, and F. Leonard, *J. Biomed. Mater. Res.*, **5**, 169 (1971).
13. S. H. Hyon, K. Jamshidi, and Y. Ikada, in *Polymers as Biomaterials*, S. W. Shalaby, Ed., Plenum Press, New York, 1984, p. 51.
14. L. Fambri, A. Pegoretti, R. Fenner, S. D. Incardona, and C. Migliaresi, *Polymer*, **38**, 79 (1996).
15. B. Eling, S. Gogolewski, and A. J. Pennings, *Polymer*, **23**, 1587 (1982).
16. J. P. Penning, H. Dijkstra, and A. J. Pennings, *Polymer*, **34**, 942 (1993).
17. S. Gogolewski and A. J. Pennings, *J. Appl. Polym. Sci.*, **28**, 1045 (1983).
18. J. W. Leenslag, S. Gogolewski, and A. J. Pennings, *J. Appl. Polym. Sci.*, **29**, 2829 (1984).
19. J. W. Leenslag and A. J. Pennings, *Polymer*, **28**, 1695 (1987).
20. A. R. Postema and A. J. Pennings, *J. Appl. Polym. Sci.*, **37**, 2351 (1989).
21. A. R. Postema, A. H. Luiten, and A. J. Pennings, *J. Appl. Polym. Sci.*, **39**, 1265 (1990).
22. A. R. Postema, A. H. Luiten, H. Oostra, and A. J. Pennings, *J. Appl. Polym. Sci.*, **39**, 1275 (1990).
23. L. Fambri, A. Pegoretti, M. Mazzurana, and C. Migliaresi, *J. Mater. Sci.: Mater. Med.*, **5**, 679 (1994).
24. I. Horáček and V. Kalíšek, *J. Appl. Polym. Sci.*, **54**, 1751 (1994).
25. I. Horáček and V. Kalíšek, *J. Appl. Polym. Sci.*, **54**, 1759 (1994).
26. I. Horáček and V. Kalíšek, *J. Appl. Polym. Sci.*, **54**, 1767 (1994).
27. O. Laitinen, P. Törmälä, R. Taurio, K. Skutnabb,

- K. Saarelainen, T. Iivonen, and S. Vainionpää, *Biomaterials*, **13**, 1012 (1992).
28. K. Jamshidi, S. H. Hyon, T. Nakamura, Y. Shimizu, and T. Teramatsu, in *Biological and Biomechanical Performance of Biomaterials*, P. Christel, A. Meunier, and A. J. C. Lee, Eds., Elsevier, Amsterdam, 1986, p. 227.
29. M. Dauner, E. Muller, B. Wagner, and H. Planck, in *Degradation Phenomena on Polymeric Biomaterials*, H. Planck, M. Dauner, and M. Renardy, Eds., Springer-Verlag, Berlin, 1992, p. 107.
30. I. Horáček and L. Kudláček, *J. Appl. Polym. Sci.*, **37**, 1 (1993).
31. A. Schindler and D. Harper, *J. Polym. Sci. Polym. Chem. Ed.*, **17**, 2593 (1979).
32. E. W. Fisher, H. J. Sterzel, and G. Wegner, *Kolloid-Z. Z. Polym.*, **251**, 980 (1973).
33. I. M. Ward, *Mechanical Properties of Solid Polymers*, 2nd ed., Wiley, Chichester, U.K., 1985, p. 334.
34. A. Pegoretti, J. Kolarik, and A. Penati, *Angew. Makromol. Chem.*, **220**, 49 (1994).
35. P. J. Flory, *J. Am. Chem. Soc.*, **67**, 2048 (1945).
36. L. E. Nielsen, *Mechanical Properties of Polymers and Composites*, Vol. 2, Marcell Dekker, New York, 1974, p. 273.
37. Y. V. Moiseev and G. E. Zaikov, *Chemical Resistance of Polymers in Aggressive Media*, Consultant Bureau, New York, 1987, p. 286.
38. H. H. Kausch, *Polymer Fracture*, Springer, Berlin, 1987, p. 69.
39. P. I. Vincent, *Polymer*, **1**, 425 (1960).
40. L. E. Nielsen, *Mechanical Properties of Polymers and Composites*, Vol. 1, Marcell Dekker, New York, 1974, p. 171.